Title Page

Mutations of *AKT3* are associated with a wide spectrum of developmental disorders including extreme megalencephaly

Authors

Diana Alcantara, Ph.D.[1], Andrew E. Timms, Ph.D.[2], Karen Gripp, M.D.[3,4], Laura Baker, M.S.[3,4], Kaylee Park, B.S.[5], Sarah Collins, M.S.[5], Chi Cheng, B.S.[5], Fiona Stewart, M.B.B.S.[6], Sarju G. Mehta, M.D.[7], Anand Saggar, M.D. [8], László Sztriha, M.D., Ph.D., DSc.[9], Melinda Zombor, M.D.[9], Oana Caluseriu, M.D., FRCPC, FCCMG[10], Ronit Mesterman, M.D., FRCPC[11], Margot I. Van Allen, M.D., MSc, FCCMG. FRCPC[12,13], Adeline Jacquinet, M.D.[14], Sofia Ygberg, M.D., Ph.D.[15], Jonathan A. Bernstein, M.D., Ph.D.[16], Aaron M. Wenger, Ph.D.[17], Harendra Guturu, Ph.D.[16], Gill Bejerano, Ph.D.[16,17], Natalia Gomez-Ospina, M.D.[16], Anna Lehmann, M.D.[18], Enrico Alfei, M.D.[19], Chiara Pantaleoni, M.D.[19], Valerio Conti, Ph.D.[20,21], Renzo Guerrini, M.D.[20,21], Ute Moog, M.D., Ph.D.[22], John M. Graham Jr., M.D., ScD.[23], Robert Hevner, M.D., Ph.D.[5,24], William B. Dobyns, M.D.[5,25], Mark O'Driscoll, Ph.D.[1], Ghayda M. Mirzaa, M.D.[5,25]

Authors' Institutional Affiliations:

[1]Genome Damage & Stability Centre, University of Sussex, Sussex, United Kingdom
[2]Center for Developmental Biology and Regenerative Medicine, Seattle Children's Research Institute, Seattle, WA
[3]Department of Pediatrics, Sidney Kimmel Medical School, Thomas Jefferson University, Philadelphia, Pennsylvania, USA
[4]Division of Medical Genetics, A.I. duPont Hospital for Children, Wilmington, Delaware, USA
[5]Center for Integrative Brain Research, Seattle Children's Research Institute, Seattle, Washington, USA
[6]Belfast Health and Social Care Trust, Belfast, Northern Ireland, United Kingdom
[7]East Anglian Medical Genetics Service, Addenbrookes Hospital, Cambridge, United Kingdom
[8]South West Thames Regional Genetic Services, St. George's NHS Trust and St. George's Hospital Medical School, London, United Kingdom
[9]Department of Pediatrics, University of Szeged, Szeged, Hungary
[10]Department of Medical Genetics, Department of Pediatrics, University of Alberta, Edmonton, AB, Canada
[11]Division of Pediatric Neurology, Developmental Pediatric Rehabilitation and Autism Spectrum Disorder, McMaster University, Hamilton, ON, Canada
[12]Department of Medical Genetics, University of British Columbia, Vancouver, Canada
[13]B.C. Children's Hospital Research Centre, Vancouver, British Columbia
[14]Center for Human Genetics, Centre Hospitalier Universitaire and University of Liège, Liège, Belgium
[15]Neuropediatric Unit and Centre for Inherited Metabolic Diseases (CMMS), Karolinska University Hospital, Stockholm, Sweden
[16]Department of Pediatrics, Stanford University School of Medicine, Stanford, California, USA
[17]Departments of Computer Science, Developmental Biology and Genetics, Stanford University School of Medicine, Stanford, California, USA

[18]Department of Medical Genetics, University of British Columbia, Vancouver, BC Canada
[19]Developmental Neurology Unit, Department of Pediatric Neurosciences, Carlo Besta Neurological Institute, IRCCS Foundation, Milan, Italy
[20]Pediatric Neurology, Neurogenetics and Neurobiology Unit and Laboratories, A. Meyer Children's Hospital, Florence, Italy
[21]IRCCS Stella Maris, Pisa, Italy
[22]Institute of Human Genetics, Heidelberg University, Heidelberg, Germany
[23]Department of Pediatrics, Cedars-Sinai Medical Center, Harbor-UCLA Medical Center, David Geffen School of Medicine Los Angeles, California, USA
[24]Department of Neurological Surgery, University of Washington, Seattle, Washington, USA
[25]Division of Genetic Medicine, Department of Pediatrics, University of Washington, Seattle, Washington, USA

Corresponding author:
Ghayda Mirzaa, M.D., Center for Integrative Brain Research, Seattle Children's Research Institute, 1900 9th Avenue, Mailstop C9S-10, Seattle, WA, USA, zip code 98101. E-mail: gmirzaa@uw.edu. Phone: 206-884-1276.

Word count: 3686

Search terms: *AKT3*, megalencephaly, polymicrogyria, hemimegalencephaly, epilepsy

Abstract

Mutations of many genes within the phosphatidylinositol-3-kinase (PI3K)-AKT-MTOR pathway are well known causes of brain overgrowth (megalencephaly) as well as segmental cortical dysplasia (such as hemimegalencephaly, focal cortical dysplasia and polymicrogyria). Mutations of the *AKT3* gene, in particular, have been reported in a few individuals with these phenotypes. However, our understanding regarding the clinical and molecular spectrum associated with mutations of this critical gene is limited, with no clear genotype-phenotype correlations. We therefore sought to further delineate this spectrum, study levels of mosaicism and identify genotype-phenotype correlations of *AKT3* related disorders. We performed targeted sequencing of *AKT3* on patients with these phenotypes by molecular inversion probes and/or Sanger sequencing to determine the type and level of mosaicism of mutations. We analyzed all clinical and brain imaging data of mutation-positive individuals including neuropathological analysis in one instance. We performed *ex-vivo* kinase assays on AKT3 engineered with the patient mutations and examined the phospholipid binding profile of Pleckstrin Homology domain localizing mutations. We identified 14 new individuals with *AKT3* mutations with several phenotypes dependent on the type of mutation and level of mosaicism. Our comprehensive clinical characterization, and review of all previously published patients, broadly segregates individuals with *AKT3* mutations into two groups: patients with highly asymmetric cortical dysplasia caused by the common p.E17K mutation, and patients with constitutional *AKT3* mutations exhibiting more variable phenotypes including bilateral cortical malformations, diffuse megalencephaly without cortical dysplasia, polymicrogyria, and periventricular nodular heterotopia. All mutations increased kinase activity, and PH domain mutants exhibited enhanced phospholipid binding. Overall, our study shows that activating mutations of the critical *AKT3* gene are associated with a wide spectrum of brain involvement ranging from focal or segmental brain malformations (such as hemimegalencephaly and polymicrogyria) predominantly due to mosaic *AKT3* mutations, to diffuse bilateral cortical malformations, megalencephaly and heterotopia due to constitutional *AKT3* mutations. We also provide the first detailed neuropathologic examination of a child with extreme megalencephaly due to a constitutional *AKT3* mutation. This child has one of the largest documented pediatric brain sizes, to our knowledge. Finally, our data show that constitutional *AKT3* mutations are associated with megalencephaly with autism, similar to *PTEN*-related disorders. Recognition of this broad clinical and molecular spectrum of *AKT3* mutations is important for providing early diagnosis and appropriate management of affected individuals, and will facilitate targeted design of future human clinical trials using PI3K-AKT pathway inhibitors.

Introduction

Mutations of multiple genes within the phosphatidylinositol-3-kinase (PI3K)-AKT-MTOR pathway are well known causes of brain overgrowth (megalencephaly) as well as segmental cortical dysplasia (such as hemimegalencephaly, focal cortical dysplasia and polymicrogyria) (Mirzaa et al., 2013). Mutations of the *AKT3* gene have been reported in eleven patients to date, including seven with constitutional mutations causing the megalencephaly-polymicrogyria-polydactyly-hydrocephalus (MPPH) syndrome (Riviere et al., 2012; Nakamura et al., 2014; Harada et al., 2015; Jamuar et al., 2014; Nellist et al., 2015; Negishi et al., 2017), and four with the mosaic p.E17K mutation causing hemimegalencephaly (Poduri et al., 2012; Riviere et al., 2012; Lee et al., 2012; Jansen et al., 2015;). However, our understanding regarding the clinical and molecular spectrum associated with mutations of this critical gene is limited, with no clear genotype-phenotype correlations. We therefore sought to further delineate this spectrum, study levels of mosaicism and identify genotype-phenotype correlations of *AKT3* related disorders. Here, we report 14 additional patients with *AKT3* mutations, including four with novel mutations, who have more diverse phenotypes including bilateral perisylvian polymicrogyria, bilateral periventricular nodular heterotopia, and megalencephaly with autism but without any cortical dysplasia. We further provide the first detailed neuropathologic characterization of extreme megalencephaly caused by a constitutional *AKT3* mutation in a previously reported child (Riviere et al., 2012). This child has one of the largest documented brain sizes in the pediatric population, to our knowledge. We also report on the first child with bilateral multifocal cortical dysplasia caused by the mosaic E17K mutation that was detectable in skin-derived DNA. Our report substantially expands the clinical, molecular and biochemical spectrum of *AKT3* related disorders and shows that activating mutations of this critical gene are associated with a broader spectrum of developmental brain disorders. Knowledge of this spectrum has important implications for the clinical and molecular diagnosis of affected individuals, recurrence risk counseling, and design of future human clinical trials using PI3K-AKT-MTOR pathway inhibitors.

Materials and methods

Human subjects and samples. The Institutional Review Board at Seattle Children's Hospital approved this study. Individuals with megalencephaly and focal malformations of cortical development were enrolled as part of the developmental brain disorders research project. Informed consent was obtained from subjects prior to enrollment in the study. Genomic DNA was extracted from various tissues (blood, saliva, skin fibroblasts, brain) using standard protocols. Brain tissue was obtained during clinically indicated epilepsy surgery and appropriate samples were analyzed by our molecular methods.

Brain Magnetic Resonance Imaging. All subjects underwent brain magnetic resonance (MR) imaging as part of their routine clinical care. The investigators reviewed all images and all relevant clinical and phenotypic data.

Statistics. p values were calculated by use of Fisher's exact test. A *P* value less than 0.05 was considered statistically significant.

Molecular methods. *Multiplex targeted sequencing using smMIPs.* We designed a pool of 26 smMIPs oligonucleotide probes targeting the coding sequences of *AKT3*. smMIPs tiled across a total of 2937 bp of genomic sequence, including 100% of the 1498 coding base pairs (bp) of *AKT3*. 100 ng capture reactions were performed in parallel. Massively parallel

sequencing was performed on an Illumina HiSeq system. Variant analysis was performed using our previously published pipeline (Mirzaa et al., 2016a). All missense, nonsense and splice site variants seen in two or more capture events that had a frequency <1% in public databases were retained for analysis.

Sanger sequencing. We performed confirmation of constitutional mutations by direct Sanger sequencing. PCR amplification was done with 50 ng of genomic DNA using Taq DNA polymerase (Applied Biosystems, Carlsbad, CA, USA). Primers used to amplify the coding and flanking non-coding regions of *AKT3* were designed using Primer 3. Double-stranded DNA sequence analysis was done with the BigDye Terminator chemistry (Applied Biosystems), and reactions were run on the ABI 3730_l Genetic Analyzer (Applied Biosystems). Sequence chromatograms were analyzed with Mutation Surveyor software version 3.30. Sequences were compared with normal control samples and the reference sequences for *AKT3*.

Overgrowth Next Generation Sequencing (NGS) panel v.1. This is multiplex PCR panel followed by NGS performed on Ion Torrent PGM platform. Allele detection limit was 1% at 1000X and 10% at 200X coverage. The threshold for mutation detection was set at 10X without strand bias.

Cell culture. HEK293 cells were grown at 37^0C in 5% CO_2 in DMEM supplemented with 10% fetal calf serum, L-GLN and antibiotics (pen-strep).

Expression vector, site-directed mutagenesis, transfection and immunoprecipitation. AKT3 expression vector was obtained from Origene (RC221051) as pCMV6-FLAG-MYC tagged Human cDNA ORF Clone containing *AKT3* (NM_005465). Patient mutations were introduced using the QuikChange® Site-Directed Mutagenesis Kit (*200518)* from Agilent Technologies (Stratagene) using custom-designed primer pairs (**Supplementary Table 1**). *AKT3* containing plasmids were expressed and transfected into HEK293 cells using calcium phosphate. Briefly, 5µg of DNA was added to 61µl of 2M $CaCl_2$ in 500µl ddH_2O. This was added drop wise to 500µl of 2x HBS (NaCl, Na_2HPO_4, HEPES pH to 7.0) before adding to adherent cells, which were harvested 48 hours later. Protein extracts were prepared by incubating the cell pellet on ice (1 hr) in detergent extraction buffer (50mM Tris.HCl pH7.5, 150mM NaCl, 2mM EDTA, 2mM EGTA, 50mM NaF, 25mM β-glycerolphosphate, 0.1mM Na-orthovanadate, 0.2% Triton-X100, 0.3% IGEPAL with protease inhibitor cocktail (Roche)). Insoluble material was precipitated by centrifugation at 4^0C and the supernatant used for immunoprecipitation. Ectopically expressed FLAG-tagged AKT3 was then immunoprecipitated using ANTI-FLAG® M2 Affinity Gel (A2220, Sigma-Aldrich) according to manufacturers' instructions.

Kinase assay. AKT3 specific kinase assay using FLAG-captured ectopically expressed AKT3 was assessed using the Nonradioactive AKT Kinase Assay Kit (9840) from Cell Signaling Technology according to manufacturers' instructions, utilizing phospho-GSK-3α/β (Ser21/9) (37F11) rabbit mAb (9327) and mouse monoclonal ANTI-FLAG® M2 antibody (F3165) from Sigma-Aldrich.

Phosphoinositide dot blot binding analysis. FLAG immunoprecipitated AKT3 was eluted from the FLAG beads using FLAG peptide (3X FLAG® Peptide, F4799 Sigma-Aldrich). PIP Strip membranes were incubated with purified AKT3 protein in 5mls of PBS-T 3%BSA according to manufacturer's instructions (P-6001 PIP STRIPS and P-6100 PIP

Array, Echelon Biosciences). Binding was detected by incubation with mouse monoclonal ANTI-FLAG® M2 antibody with chemiluminesence detection.

Results

Clinical results. We identified *AKT3* mutations in 14 new, and four previously reported, subjects, who collectively demonstrate a wide spectrum of features (Jansen et al., 2015; Nellist et al., 2015; Riviere et al., 2012). The clinical and molecular data of our 13 new mutation-positive children, as well as the previously published nine patients, are summarized in **Table 1**. The neuroimaging features of these children are shown in **Fig. 1.** More comprehensive clinical, neuroimaging and molecular data provided in **Supplementary Tables 2-5**.

Neuroimaging features. First, we identified the mosaic p.E17K *AKT3* mutation in three children. The first child (LR15-262) had hemimegalencephaly with contralateral hemimicroencephaly (**Fig. 1A-B**), and several cutaneous capillary malformations. This child was born in status epilepticus, had early onset intractable epilepsy, and underwent hemispherectomy at age two weeks. The second patient (LR16-251) harboring the p.E17K mutation had a distinctive phenotype characterized by megalencephaly with multifocal but bilateral cortical dysplasia (**Fig. 1C-D**). This child had intractable epilepsy and passed away at the age of 10 months due to his deteriorating neurologic status. He also had three capillary-lymphatic malformations. The third child (LR11-443) had a massively enlarged and dysplastic cerebral hemisphere with dysplasia identified in the contralateral hemisphere as well. She also had a distinctive vascular malformation on the lower leg characterized by cutis marmorata telangiectatica congenita (or CMTC) (Jansen et al., 2015).

Second, we identified constitutional *AKT3* mutations in the remaining 14 patients who can be clinically segregated into three groups. The first group includes children with megalencephaly and polymicrogyria (PMG) (N = 6). These children had bilateral perisylvian polymicrogyria with variable ventriculomegaly (**Fig. 1K-R**). Among this group, one child had hydrocephalus requiring neurosurgical shunting and Chiari malformation requiring posterior fossa decompression (LR14-254; **Fig. 1O-P**). This child showed global psychomotor delay at two years of age (due to mainly langue and motor delays). However, on preschool evaluation at age six years, he showed normal cognitive skills (Wechsler Preschool and Primary Scale of Intelligence, WPPSI, score =92). The second group consists of children with megalencephaly and diffuse cortical dysplasia (also termed dysplastic megalencephaly, or DMEG) with diffuse and bilateral periventricular nodular heterotopia, a rare subgroup not previously associated with any genes (N=3) (**Fig. 1G-J, W-X**). Patients LR16-301 and LP96-103 had extensive heterotopia all along the ventricular surface (**Fig. 1G-J**), whereas patient LR14-112 had fewer and more discrete heterotopia (**Fig. 1W-X**). Interestingly, all three patients within this group had moderate to severe ventriculomegaly. The third group of children with constitutional mutations had megalencephaly with no or subtle (often unilateral) cortical malformations and variable ventriculomegaly (N = 4) (**Fig. 1E-F, S-V**). One child within this group had megalencephaly, mildly thick corpus callosum and very subtle cortical dysplasia with unilateral prominent in cortical infolding into the perisylvian region (LR12-470, **Fig. 1, S-T**). This child had mild learning issues and communication problems. Another child within this group (LR13-008) was formally diagnosed with Autism Spectrum Disorders (ASD). Finally, one child (LR17-XXX) within this group as well had megalencephaly alone with normal tone, and no developmental or neurologic issues at age three years (**Supplementary Data**).

Neuropathologic abnormalities. We examined the neuropathologic features of megalencephaly-associated polymicrogyria in a previously reported *AKT3* mutation-positive child (LR08-018) who died unexpectedly at age six years. This boy had congenital megalencephaly, bilateral perisylvian polymicrogyria, cerebellar tonsillar ectopia, somatic asymmetry and connective tissue dysplasia (Mirzaa et al., 2012). He was identified to have a *de novo* p.R465W mutation in *AKT3* (Riviere et al., 2012). This child passed away during sleep presumably due to Sudden Unexpected Death in Epilepsy (SUDEP) (further details provided in the **Supplementary Text**). Neuropathologic analysis on postmortem brain tissue revealed that his brain weighed twice the normal weight of adult brains (total weight = 2313 gms) and was asymmetrically enlarged (**Fig. 2A-B**). There was evidence of diffuse cortical dysplasia with irregular hyperconvoluted gyri suggestive of diffuse polymicrogyria, including anomalous branching and fusion of gliotic layer 1. There were also increased numbers of neurons in layer 6 and within the white matter that appeared disorganized and maloriented. However, neurons were not strikingly enlarged or dysplastic, and no balloon cells were identified. The hippocampus was grossly small and gliotic, and the dentate gyrus exhibited focal "tram-track" splitting of the granule cell layer, typically associated with chronic epilepsy (**Fig. 2B-Q**).

Somatic features. Several children in this series had vascular malformations including cutis marmorata telangiectatica congenita (LR11-443), capillary malformations and/or prominent veins (N = 4), and connective tissue abnormalities including aplasia cutis congenita (N = 2). One child (LR13-008) had a prenatal stroke due to occlusion of the right cerebral artery, with no evidence of thrombophilia. Several patients had endocrine issues including recurrent hypoglycemia (N = 2) and hypothyroidism (N = 1). Other notable features include immunologic issues including recurrent infections (N = 2). In one of these patients (LR14-112), recurrent infections were due to combined IgA and IgE deficiency. Patient LR13-008 also had severe vitamin A malabsorption (**Supplementary Table 4**).

Molecular results. All 14 *AKT3* mutations reported in this series, and our previously reported four mutations, were identified or confirmed by targeted Next Generation and/or Sanger sequencing. Levels of mosaicism, tissues tested and methods of detection are provided in **Supplementary Table 5**. Mutations in two children with megalencephaly and megalencephaly with heterotopia (LR16-372 and LR16-301) were identified by clinical whole exome sequencing (WES) on the proband, followed by targeted parental mutation analysis by Sanger sequencing.

The p.E17K mutation detected in our three patients was low-level mosaic, as mentioned previously. In LR15-262, the alternate allele percentage (AAP) was 12.6-13.9% in affected brain tissue from the more dysplastic hemisphere resected during epilepsy surgery. Interestingly, the mutation was detectable in skin fibroblasts from normal-appearing skin (at 8.6-9.5% AAP) but was undetectable in peripheral blood-derived DNA. The mutation in patient LR11-443 was present in 20-36% of cells from several affected brain regions form the more severely affected hemisphere. It was also detectable at a very low level (1.3% of alleles) from skin fibroblast-derived DNA (also from healthy-appearing skin). In LR16-251 who had bilateral multi-focal cortical dysplasia, the p.E17K mutation was present at a very low level in skin fibroblasts (AAP 1.8%). This child did not undergo epilepsy surgery due to his bilateral malformations, and no postmortem brain tissue was available for molecular analysis. The other *AKT3* mutations identified in our series were all constitutional, and were confirmed to be *de novo* when parental DNA was available. Five novel constitutional *AKT3* mutations –

p.N53L, p.F54Y, p.V268A, p.D322N, and p.W79C – were detected in five children in this series. Mutations in two patients (LR12-470 and LR13-008) are presumed to be constitutional as DNA derived from saliva was used for molecular analysis, and peripheral blood-derived DNA was unavailable.

Functional analysis of *AKT3* mutants. With the exception of p.R465W, which localizes to the C-terminal region of AKT3, the remaining mutations were found in the Pleckstrin homology (PH) domain or the catalytic kinase domain (**Fig. 3A**). Kinase activity analysis following ectopic over-expression clearly showed that all identified patient mutations caused increased activity compared to wild-type (WT) AKT3 (**Fig. 3, B-C**). The p.E17K PH mutant domain has previously been shown to result in elevated kinase activity and to be oncogenic via enhanced pathological localization to the plasma membrane (Carpten et al., 2007; Parikh et al., 2012). As the PH domain is critical for phospholipid binding and consequent kinase activation, we assessed whether the novel mutations localized in the PH domain described here (p.N53K and p.F54Y) have a similar impact upon phospholipid binding as p.E17K (Parikh et al., 2012; Park et al., 2008). We employed dot-blot analysis using an array of different phospholipids immobilized on WT AKT3. Indeed, these PH mutant domains exhibited markedly elevated binding to phosphatidylinositol (3,4) biphosphate (PtdIns(3,4)P_2) in particular, which is a key plasma membrane constituent and substrate of phosphatidylinostitol-3-kinase.

Discussion

Malformations of cortical development (MCDs) comprise a wide range of disorders characterized by aberrant neuronal migration, proliferation and organization, and result in significant childhood morbidity and mortality (Barkovich et al., 2012). A growing spectrum of these malformations is now known to be caused by germline or mosaic mutations of genes within the PI3K-AKT-MTOR signaling network (Jamuar et al., 2014; Mirzaa et al., 2013; Mirzaa and Poduri, 2014). The post-zygotic (mosaic) mutations are most readily identified in affected (surgically removed) brain tissues (Mirzaa et al., 2016b).

AKT3 is one of three AKT homologues (AKT1,2,3), the central effector of the PI3K-AKT-MTOR pathway (Yang et al., 2004). Mutations of *AKT1* and *AKT2* have been identified in somatic overgrowth disorders such as Proteus syndrome and in somatic overgrowth with hypoglycemia, respectively (Hussain et al., 2011; Lindhurst et al., 2011). Reported children with these phenotypes to date all harbored the p.E17K mutation in these respective genes. The paralogous mutation in the brain-enriched isoform, *AKT3*, has been identified in mosaic form in children with hemimegalencephaly (HMEG) (Jansen et al., 2015; Poduri et al., 2012). Constitutional mutations of *AKT3* have been identified in children with diffuse megalencephaly in syndromic forms such as the megalencephaly-polymicrogyria-polydactyly-hydrocephalus (MPPH) syndrome, and somatic duplications of the *AKT3* locus have been identified in a few children with HMEG and diffuse megalencephaly (MEG) without cortical dysplasia (Chung et al., 2014; Conti et al., 2015; Hemming et al., 2016; Wang et al., 2013). To date, only nine children (with four mutations) have been reported with *AKT3* mutations. Here, we report on the clinical and neuroimaging spectrum of 13 children identified to have constitutional or mosaic *AKT3* mutations, including five children with four novel *AKT3* mutations, adding to our previously published data on four *AKT3* mutation-positive children (Jansen et al., 2015; Nellist et al., 2015; Riviere et al., 2012). Using in vitro kinase assay, we show that these mutations constitutionally activate AKT3.

Our series provides several important insights into the clinical and molecular spectrum of mutations associated with this critical gene. First, our series shows that there are important and emerging genotype-phenotype correlations of AKT3 mutations whereby highly mosaic p.E17K mutation is associated with very segmental brain malformations (i.e. HMEG), whereas constitutional mutations are associated with more widespread cortical malformations with bilateral (but often asymmetric) findings. We describe two new patients with the recurrent, mosaic p.E17K mutation. Importantly, one of these children had a novel phenotype characterized by multifocal and bilateral focal cortical dysplasia lacking a severity gradient between right and left hemispheres, unlike all previously reported children with the E17K *AKT3* mutation who had highly asymmetric cortical dysplasia (regarded as "classic hemimegalencephaly"). Second, our series substantially broadens the clinical spectrum of constitutional *AKT3* mutations to include diffuse, most often perisylvian, polymicrogyria (PMG) and periventricular nodular heterotopia (PNH), with hydrocephalus and cerebellar tonsillar ectopia occurring in a subset of individuals. Therefore, this report presents *AKT3* mutations as the first genetic cause of MEG with PNH and PMG; a clinical phenotype previously reported as a distinct entity (Wieck et al., 2005). Importantly, our series further shows that constitutional AKT3 mutations, which can also occur in the PH domain where p.E17K mutation localizes, are associated with diffuse MEG without cortical malformations, with normal cognitive development in one patient who had autistic features – resembling the PTEN-hamartoma tumor syndrome and suggesting that mutations of the AKT3 gene are associated with Autism Spectrum Disorders (ASD).

Collectively our data suggest that there are several distinct brain malformation syndromes caused by *AKT3* mutations that can be broadly categorized into: (1) highly segmental cortical dysplasia (including HMEG) and vascular malformations associated with the mosaic E17K *AKT3* mutation. We believe that this comprises a clinically recognizable subgroup with MEG, extensive focal cortical dysplasia (either HMEG or bilateral, multifocal FCD), and cutaneous vascular malformations; (2) MEG-PMG with frequent asymmetry and occasionally patchy somatic findings (as occurs in MPPH syndrome); (3) MEG-PMG with periventricular nodular heterotopia (PNH); and (4) MEG with normal or minimal cortical dysplasia, and ASD or autistic features (**Fig. 4**). We believe this clinical stratification is diagnostically important as resection of epileptic brain tissue is likely to be clinically warranted for children in group 1, but less likely in groups 2-3. Hydrocephalus and Chiari malformations, on the other hand, are complications likely to occur in children with diffuse MEG occurring in groups 2-3, depending on the severity of ventriculomegaly and cerebellar tonsillar enlargement, respectively.

Seizures are a common feature of our cohort and have been reported in *Akt* mouse models with activating *Akt3* mutations (Baek et al., 2015; Tokuda et al., 2011). Seizures are especially severe in children with the E17K mutation, likely due to the severity of the underlying cortical malformation. However, one of our patients (LR08-018) with the constitutional R465W *AKT3* mutation had intractable epilepsy as well, and may have had SUDEP; an interesting association that suggests that aggressive anti-epilepsy treatment and management may be necessary this spectrum. This association will require further investigation in future children identified to have *AKT3* mutations.

With regards to non-neurologic findings, our series shows that vascular malformations (VM) are common with *AKT3* related disorders and may provide useful diagnostic clues. VM in all *AKT3* mutation patients reported to date were patchy, few, and best characterized as capillary malformations, although one patient (LR11-443) had cutis marmorata telangiectatica

congenita (CMTC), which is clinically distinct from capillary malformations. Unlike *PIK3CA* related disorders, these VMs were not associated with marked somatic overgrowth, lipomatosis, or soft tissue hypertrophy (Keppler-Noreuil et al., 2015; Mirzaa et al., 2016a). The occurrence of a prenatal stroke in one child is clinically noteworthy, as prenatal strokes and/or thrombophilia have been reported in some children with the megalencephaly-capillary malformation syndrome (MCAP) caused by *PIK3CA* mutations, as well as in Proteus syndrome caused by *AKT1* mutations (Mirzaa et al., 2012; Slavotinek et al., 2000).

Two children in our series also had hypoglycemia. These data add to a previous report of hypoglycemia with *AKT3* related disorders and further support this gene's roles in glucose regulation (Nellist et al., 2015). Mutations of *AKT2* are known to cause asymmetric overgrowth with hypoglycemia, exemplifying the critical role of this gene in insulin-dependent glucose regulation (Arya et al., 2014; Cho et al., 2001; Garg et al., 2015; Hussain et al., 2011). While the cause of hypoglycemia in our patients remains undetermined, this potential association warrants further studies as this may have important clinical implications for *AKT3* mutation-positive children identified in the future as well.

Our functional analysis of each of the patient mutations showed a robust elevation of catalytic kinase activity. This is consistent with the elevated PI3K-AKT-MTOR signaling underlying these types of brain overgrowth disorders. Furthermore, PH domain-localizing mutations all exhibited elevated phospholipid binding compared to wild type (WT). This feature of the p.E17K mutation has been proposed to explain why this mutation is oncogenic and recurrent in a wide range of cancers (Carpten et al., 2007)**.** Considering the similar phospholipid binding profile, we have uncovered here for p.N53K and p.F54Y compared to p.E17K, our findings suggest that careful monitoring of such individuals in particular for cancers is warranted, although formal cancer surveillance guidelines cannot be proposed at this time due to lack of clinical evidence of these complications.

In summary, we show that activating mutations of *AKT3* are associated with a much broader spectrum of developmental brain disorders in children, with several clinical phenotypes determined partially by the type of mutation and level of mosaicism. Our series suggests that the mosaic E17K *AKT3* mutation is associated with highly segmental brain malformations that may warrant surgical resection to achieve seizure control, whereas constitutional mutations of *AKT3* are associated with bilateral brain malformations including bilateral perisylvian polymicrogyria, periventricular nodular heterotopia and megalencephaly without cortical dysplasia. In this series, we also report on the neuropathologic abnormalities caused by a constitutional *AKT3* mutation in one of the largest documented brain sizes in the pediatric population. Our data also suggest that monitoring for hypoglycemia in affected individuals may be warranted as well.

Acknowledgements
We thank the patients, their families and referring providers for their contribution and support of our research. We thank Dr. Louanne Hudgins from the Department of Pediatrics at Stanford University School of Medicine for her collaboration and for providing clinical data.

Funding

Research reported in this publication was supported by the National Institute of Neurological Disorders and Stroke (NINDS) and the National Heart, Lung and Blood Institute (NHLBI) and the National Institutes of Health (NIH) under award numbers K08NS092898 (to G.M.), R01NS092772 and R01HL130996 (to W.B.D.), a Cancer Research UK Programme award C24110/A15394 (to M.O'D.) and grant N602531 from the European Union Seventh Framework Program under project DESIRE (to R.G.); and RF-2013-02355240 (to R.G.).

The content is solely the responsibility of the authors, and does not necessarily represent the official views of the National Institutes of Health. The funding sources had no role in the design and conduct of the study, collection, management, analysis and interpretation of the data, preparation, review or approval of the manuscript, or decision to submit the manuscript for publication.

Disclosure
The authors report no disclosures relevant to the manuscript.

Tables

Table 1. Summary of the clinical and molecular findings of *AKT3* mutation-positive patients (N=24) [AKT3: NM_005465.4]

Subject ID	Diagnosis	cDNA change	Amino acid change	Functional domain	Inheritance	Mutation type, AAP (tissue)
Mosaic *AKT3* mutations (N=5)						
LR15-262	DMEG/HMEG	c.49G>A	p.Glu17Lys	PH	NA	Mosaic, ~8-14% (brain, skin)
HME-1565 (Lee et al., 2012)	HMEG	c.49G>A	p.Glu17Lys	PH	*De novo*	Mosaic, ~16-30% (brain)
Patient 3 (Poduri et al., 2012)	DMEG/HMEG	c.49G>A	p.Glu17Lys	PH	*De novo*	Mosaic, 35% (brain)
LR11-443 (Jansen et al., 2015)	DMEG/HMEG	c.49G>A	p.Glu17Lys	PH	*De novo*	Mosaic, 1-18% (brain, skin)
LR16-251	DMEG/multifocal	c.49G>A	p.Glu17Lys	PH	NA	Mosaic, 1.8% (skin)
Constitutional *AKT3* mutations (by functional domain; N=19)						
Patient (Takagi et al., 2017)	MEG	c.118G>A	p.Glu40Lys	PH	*De novo*	Constitutional
LR16-372	MEG	c.159C>A	p.Asn53Lys	PH	*De novo*	Constitutional
LR16-301	MEG-PMG-PNH	c.161T>A	p.Phe54Tyr	PH	*De novo*	Constitutional
LR17-XXX	MEG	c.237G>T	p.Trp79Cys	PH	*De novo*	Constitutional
LP96-103	MEG-PMG-PNH	c.548T>A	p.Val183Asp	Kinase	*De novo*	Constitutional
LR12-314 (Nellist et al., 2015)	MEG-PMG-PNH	c.548T>A	p.Val183Asp	Kinase	*De novo*	Constitutional
LR11-354 (Riviere et al., 2012)	MEG-PMG	c.686A>G	p.Asn229Ser	Kinase	*De novo*	Constitutional
Patient (Harada et al., 2015)	MEG-PMG	c.686A>G	p.Asn229Ser	Kinase	*De novo*	Presumed constitutional[a]
Patient 2 (Nakamura et al., 2014)	MEG-PMG [MCAP]	c.686A>G	p.Asn229Ser	Kinase	*De novo*	Constitutional

Patient 1 (Negishi et al., 2014)	MEG-PMG	c.686A>G	p.Asn229Ser	Kinase	*De novo*	Constitutional
LR13-041	MEG-PMG	c.803T>C	p.Val268Ala	Kinase	*De novo*	Presumed constitutional[a]
LR14-271	MEG-PMG	c.964G>A	p.Asp322Asn	Kinase	*De novo*	Constitutional
LR14-254	MEG-PMG	c.964G>A	p.Asp322Asn	Kinase	*De novo*	Constitutional
LR12-412	MEG-PMG	c.1393C>T	p.Arg465Trp	C-terminal	NA	Constitutional
LR14-025	MEG-PMG	c.1393C>T	p.Arg465Trp	C-terminal	*De novo*	Constitutional
LR12-470	MEG	c.1393C>T	p.Arg465Trp	C-terminal	*De novo*	Presumed constitutional[a]
LR13-008	MEG-autism	c.1393C>T	p.Arg465Trp	C-terminal	*De novo*	Presumed constitutional[a]
LR14-112	MEG-PMG-PNH	c.1393C>T	p.Arg465Trp	C-terminal	*De novo*	Constitutional
LR08-018 (Riviere et al., 2012)	MEG-PMG	c.1393C>T	p.Arg465Trp	C-terminal	*De novo*	Constitutional
PMG-3801 (Jamuar et al., 2014)	MEG-PMG	c.1393C>T	p.Arg465Trp	C-terminal	*De novo*	Constitutional

Abbreviations: AAP, alternative allele percentage (i.e. mutation level); DMEG, dysplastic megalencephaly; HMEG, hemimegalencephaly; MEG, megalencephaly; MPPH, megalencephaly-polymicrogyria-polydactyly-hydrocephalus syndrome; NA, not available; PNH, periventricular nodular heterotopia; PMG, polymicrogyria.

[a]Mutations are presumed to be constitutional or germline due to one tissue only being analyzed, with no evidence of mosaicism in the analyzed tissue

Figures and figure legends

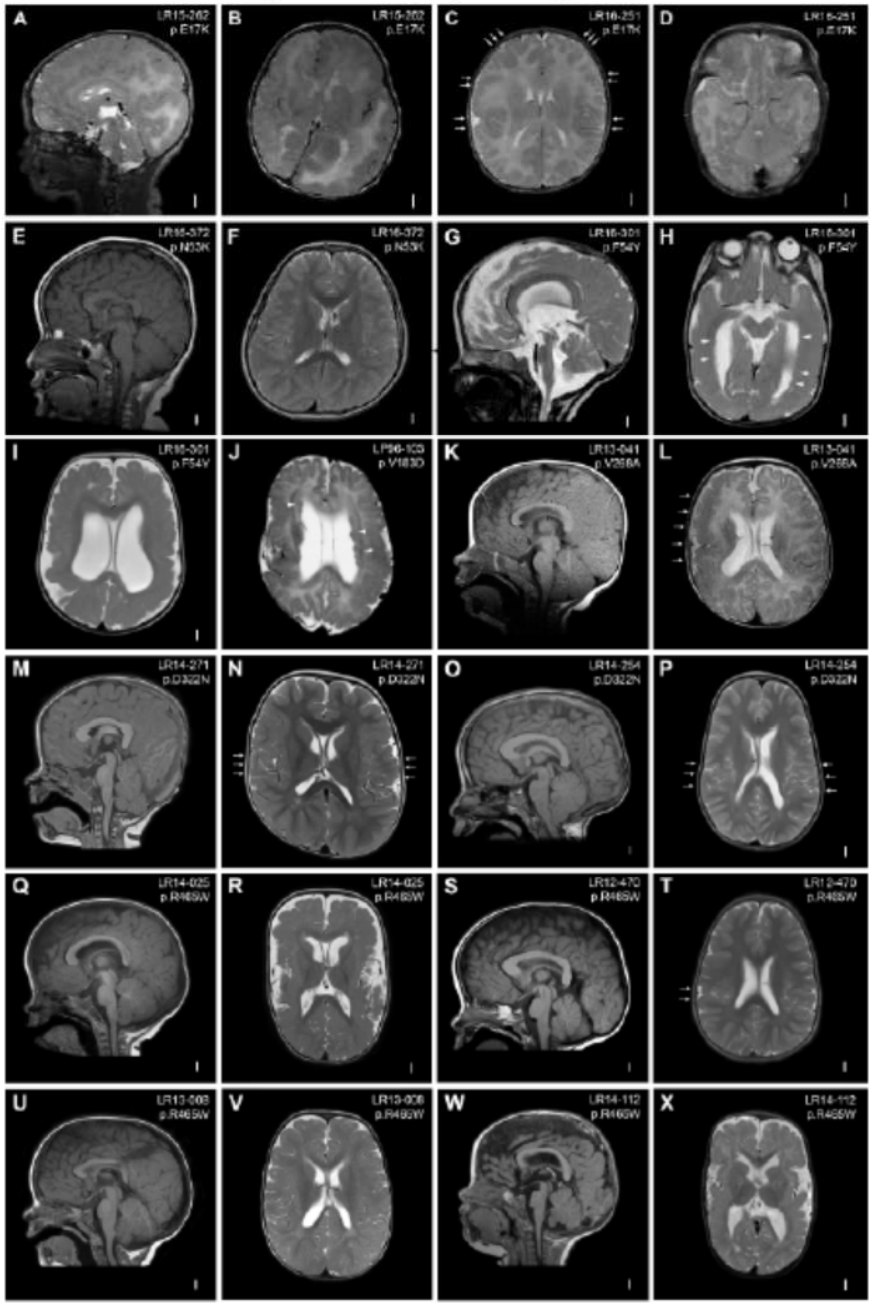

Figure 1. Brain MRIs of *AKT3* mutation-positive children. A-B, Brain MR images of patient LR15-262 showing markedly enlarged and dysplastic right cerebral hemisphere with diffuse cortical dysplasia and dysmyelination consistent with hemimegalencephaly. The contralateral hemisphere is markedly decreased in size with areas of cortical dysplasia (hemimicroencephaly); **C-D**, images of patient LR16-251 showing multifocal areas of dysplastic cortex in the perisylvian, frontal, temporal and occipital regions (arrows); **E-F**, images of patient LR16-372 showing a thick and dysplastic corpus and deeply in folded perisylvian regions; **G-I**, images of patient LR16-301 showing striking megalencephaly, ventriculomegaly, stretched but thick

corpus callosum, diffuse polymicrogyria with deep in folding in the right occipital lobe, and bilateral periventricular nodular heterotopia (arrowheads); **J**, image of patient LP96-103 showing diffuse bilateral perisylvian polymicrogyria, ventriculomegaly, cavum septum pellucidum et vergae and diffuse periventricular nodular heterotopia (arrowheads); **K-L**, images of patient LR13-041 showing a large cerebellum with cerebellar tonsillar ectopia, bilateral polymicrogyria predominantly in the perisylvian region (more severe on the right, arrows) with dysmyelination; **M-N**, images of patient LR14-271 showing diffuse megalencephaly with a thick corpus callosum and deep infolding in the perisylvian region suggestive of polymicrogyria (arrows); **O-P**, images of patient LR14-254 showing diffuse megalencephaly, thick corpus callosum and bilaterally diffuse infolding of the perisylvian region suggestive of polymicrogyria (arrows); **Q-R**, images of patient LR14-025 showing megalencephaly, thick corpus callosum and bilateral diffuse polymicrogyria with increased extra-axial space; **S-T**, images of patient LR12-470 showing megalencephaly and thick corpus callosum. This patient also had deep infolding in the right perisylvian region suspicious for polymicrogyria, with very limited involvement (arrows); **U-V**, images of patient LR13-008 showing diffuse megalencephaly and possible area of cortical dysplasia in the right perisylvian region; **W-X**, images of patient LR14-112 showing diffuse megalencephaly, bilateral perisylvian polymicrogyria and bilateral ventriculomegaly.

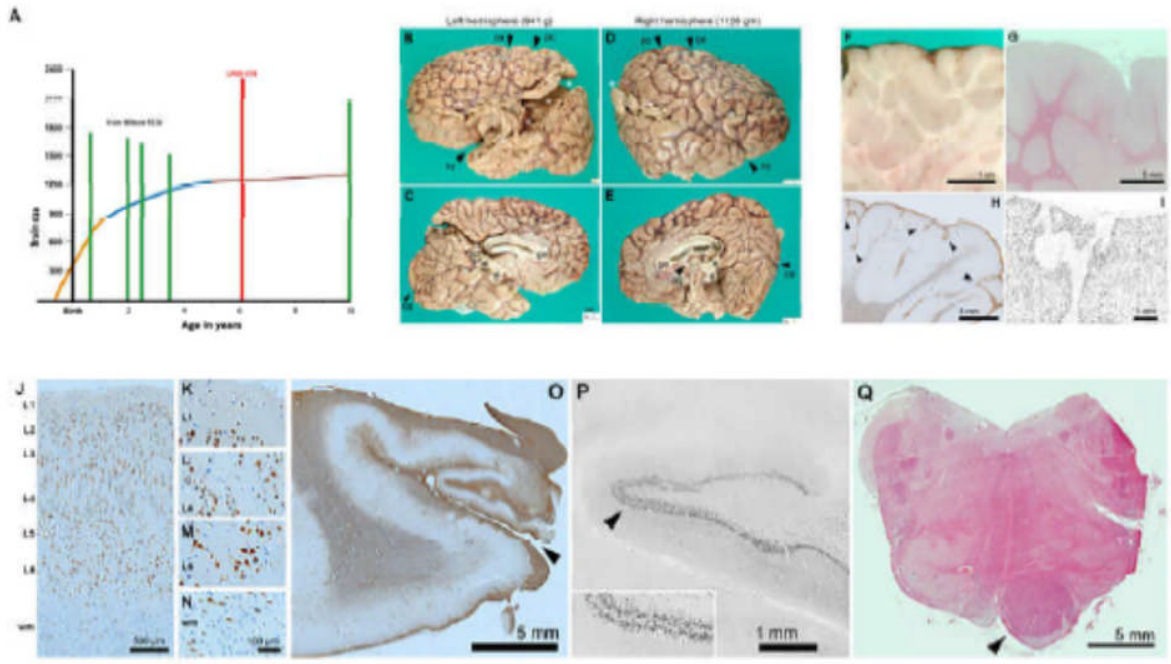

Figure 2. Pathologic examination of the brain of patient LR08-018 (p.R465W).
A, Brain size. Graph depicting the largest pediatric brain sizes (in grams) previously reported in the literature (green bars) in relationship to the brain size of patient LR08-018 (with the p.R465W mutation, red bar) demonstrating that brain size for this patient is markedly larger than these patients (Wilson, 1934). The graph is an adaptation of the human brain growth diagram from the Smithsonian Institute (http://humanorigins.si.edu/human-characteristics/brains). The graph shows the periods of rapid brain growth (in orange) plus the period of decreased brain growth (in blue) followed by the plateau in brain growth.

B-E, Cerebral hemispheres. The massive brain (2313 g; approximately twice normal weight for age) was asymmetrically enlarged. The left hemisphere (B, C) weighed 941 g, and the right (D, E) weighed 1128 g. Primary fissures such as the Sylvian (sy), central (ce), postcentral (pc), and calcarine (ca) sulci were recognizable, but secondary and tertiary sulci were abnormal. Gyri appeared irregular and overall hyperconvoluted. The corpus callosum was present including genu (ge), body, and splenium (sp). The anterior commissure (ac) was present but small. White asterisks: artefactual disruption of hemispheres due to brain removal and transport. Black asterisks: torn junction of hemispheres and midbrain. All panels at same magnification.

F-I. Hyperconvolution and polymicrogyria in cerebral cortex. (F) Brain slice through parietal cortex showed redundant folds of cortex extending deep into white matter. (G) Histological section (H&E) through the same region showed relatively sharp gray-white junctions. (H) Inferior temporal cortex exhibited features of polymicrogyria, including anomalous branching and fusion of gliotic layer 1 (GFAP immunohistochemistry). (I) Layer 1 fusion and branching were confirmed by NeuN immunohistochemistry.

J-N. Abnormal layering of cerebral cortex, and excessive white matter neurons. In foci not involved by polymicrogyria, such as right posterior perisylvian cortex, cortical layering was moderately disorganized. (J) Cortical layers were identified based on cell size and density. NeuN immunohistochemistry. (K) Layer 1 was cell-sparse and contained only small neurons. (L) Layer 4 contained typical small (granular) neurons. (M) Layer 6 neurons were particularly disorganized and maloriented. (N) Increased neurons in white matter (wm). Interestingly, neurons in this case were not strikingly enlarged or dysplastic, nor were any balloon cells present.

O-Q. Hippocampal and brainstem abnormalities of patient LR08-018. (O) The left hippocampus was very small and gliotic, and the hippocampal sulcus (arrowhead) was open, suggesting a deficiency of perforant pathway fibers, which would normally cross the fused sulcus. GFAP immunohistochemistry. (P) Histologically, the dentate gyrus exhibited focal "tram-track" splitting of the granule cell layer (arrowhead; enlarged 2X in inset), a finding usually associated with chronic epilepsy. (Q) The upper medulla showed marked asymmetry of the pyramidal tract, essentially limited to one side (arrowhead). The adjacent inferior olives were moderately hypoconvoluted. H&E.

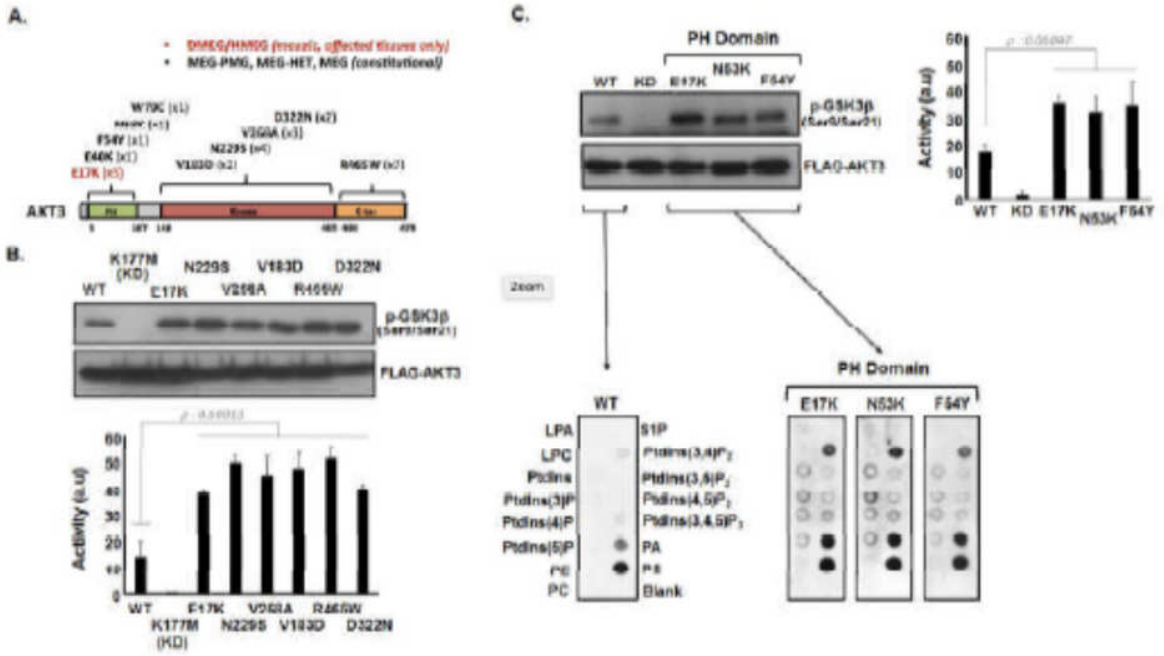

Figure 3. Analysis of AKT3 activity *in vitro.*
A, The primary structure of AKT3 showing the relative positions of the Pleckstrin Homology (PH) domain for lipid binding the catalytic kinase domain and C-terminal (C-ter) region. Mutations identified to date are shown along with the numbers of patients with these mutations in brackets. **Abbreviations:** DMEG, dysplastic megalencephaly; HMEG, hemimegalencephaly; MEG, megalencephaly; MPPH, megalencephaly-polydactyly-hydrocephalus (MPPH) syndrome.

B, Catalytic kinase domain and C-terminal localizing patient-derived *AKT3* mutations are associated with elevated kinase activity. Ectopically expressed wild-type (WT) AKT, a kinase dead variant K177M, the E17K activating PH domain mutant and various patient mutants were assessed for kinase activity using a GSK3β peptide as a substrate in an *ex vivo* kinase assay. The upper panel shows immune detection of phosphorylated GSK3β peptide following western blotting with anti-phospho-GSK3β (Ser9/Ser21) antibody. The patient mutants all exhibit elevated phospho-activity compared to WT. The graph depicts quantitation of phospho-GSK3β (Ser9/Ser21) signal (a.u. arbitrary units). Error bars represent mean ± SD (n=4), p-values were determined using Student's *t*-test.

C, PH domain localizing patient mutations are associated with elevated kinase activity and altered phospholipid-binding profile. Left-hand panels show western blot analysis of phospho-GSK3β (Ser9/Ser21) of ectopically expressed wild-type (WT), K177M kinase dead and three PH domain patient mutants; E17K, N53K and F54Y. The graph depicts quantitation of phospho-GSK3β (Ser9/Ser21) signal (a.u. arbitrary units). Error bars represent mean ± SD (n=4), p-values were determined using Student's *t*-test.

The bottom panels depict PIP-membranes seeded with various lipids and phospholipids for dot blot binding analysis. Ectopically expressed FLAG-tagged WT and AKT3 PH domain mutants were incubated with the PIP Strips and bound protein detected by western blotting using anti-FLAG. All three PH domain mutants exhibit altered and elevated binding to specific phospholipids compared to WT. LPA; Lysophophatidic acid, S1P: Sphingosine-1-phosphate, LPC; Lysophosphocholine, PtdIns; Phosphatidylinositol, P; phosphate, PE; Phosphatidylethanolamine, PA; Phosphatidic acid, PS; Phosphatidylserine, PC; Phosphatidylcholine.

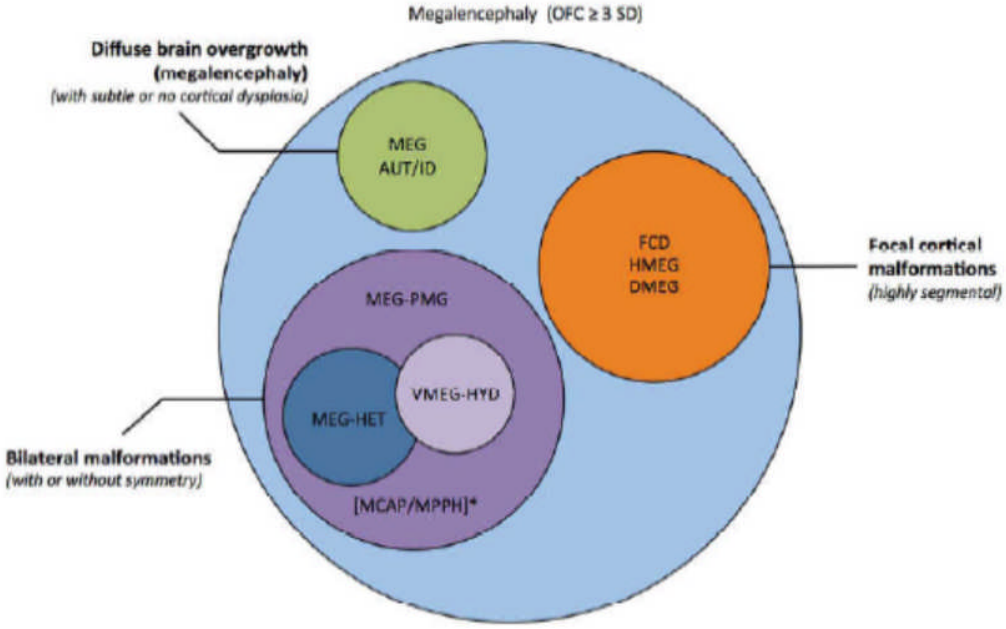

Figure 4. Diagram showing the spectrum of *AKT3* associated phenotypes. Several groups of partially overlapping developmental brain disorders are associated with *AKT3* mutations that include the following phenotypes (1) focal malformations of cortical development that are highly segmental (e.g. FCD, HMEG, DMEG; orange); (2) bilateral polymicrogyria (PMG, dark purple) with or without ventriculomegaly or hydrocephalus (VMEG-HYD; light purple), and heterotopia (HET; blue); (3) diffuse megalencephaly (MEG) with intellectual disability (ID) and/or Autistic features (AUT) with subtle or no cortical dysplasia (green). *Of note, the megalencephaly-capillary malformation syndrome (MCAP) and the megalencephaly-polymicrogyria-polydactyly-hydrocephalus syndrome (MPPH) fit within the second group of *AKT3* related disorders, from the brain phenotype perspective. MCAP can be further clinically distinguished by somatic findings (somatic overgrowth, vascular or lymphatic abnormalities), and MPPH by the occurrence of polydactyly in a subset of affected individuals.

Abbreviations: AUT, autism; DMEG, dysplastic megalencephaly; FCD, focal cortical dysplasia; HET, heterotopia; HMEG, hemimegalencephaly; HYD, hydrocephalus; PMG, polymicrogyria; VMEG, ventriculomegaly.

References

Arya, V.B., et al., 2014. Activating AKT2 mutation: hypoinsulinemic hypoketotic hypoglycemia. J Clin Endocrinol Metab. 99**,** 391-4.

Baek, S.T., et al., 2015. An AKT3-FOXG1-reelin network underlies defective migration in human focal malformations of cortical development. Nat Med. 21**,** 1445-1454.

Barkovich, A.J., et al., 2012. A developmental and genetic classification for malformations of cortical development: update 2012. Brain. 135**,** 1348-69.

Carpten, J.D., et al., 2007. A transforming mutation in the pleckstrin homology domain of AKT1 in cancer. Nature. 448**,** 439-444.

Cho, H., et al., 2001. Insulin resistance and a diabetes mellitus-like syndrome in mice lacking the protein kinase Akt2 (PKB beta). Science. 292**,** 1728-31.

Chung, B.K., et al., 2014. Duplication of AKT3 is associated with macrocephaly and speech delay. Am J Med Genet A. 164a**,** 1868-9.

Conti, V., et al., 2015. Focal dysplasia of the cerebral cortex and infantile spasms associated with somatic 1q21.1-q44 duplication including the AKT3 gene. Clin Genet. 88**,** 241-7.

Garg, N., et al., 2015. MORFAN Syndrome: An Infantile Hypoinsulinemic Hypoketotic Hypoglycemia Due to an AKT2 Mutation. J Pediatr. 167**,** 489-91.

Harada, A., et al., 2015. Sudden death in a case of megalencephaly capillary malformation associated with a de novo mutation in AKT3. Childs Nerv Syst. 31**,** 465-71.

Hemming, I.A., et al., 2016. Reinforcing the association between distal 1q CNVs and structural brain disorder: A case of a complex 1q43-q44 CNV and a review of the literature. Am J Med Genet B Neuropsychiatr Genet. 171b**,** 458-67.

Hussain, K., et al., 2011. An activating mutation of AKT2 and human hypoglycemia. Science. 334**,** 474.

Jamuar, S.S., et al., 2014. Somatic mutations in cerebral cortical malformations. N Engl J Med. 371**,** 733-43.

Jansen, L.A., et al., 2015. PI3K/AKT pathway mutations cause a spectrum of brain malformations from megalencephaly to focal cortical dysplasia. Brain. 138**,** 1613-28.

Keppler-Noreuil, K.M., et al., 2015. PIK3CA-related overgrowth spectrum (PROS): diagnostic and testing eligibility criteria, differential diagnosis, and evaluation. Am J Med Genet A. 167a**,** 287-95.

Lee, J.H., et al., 2012. De novo somatic mutations in components of the PI3K-AKT3-mTOR pathway cause hemimegalencephaly. Nat Genet. 44(8):941-5.

Lindhurst, M.J., et al., 2011. A mosaic activating mutation in AKT1 associated with the Proteus syndrome. N Engl J Med. 365**,** 611-9.

Mirzaa, G., et al., 2016a. PIK3CA-associated developmental disorders exhibit distinct classes of mutations with variable expression and tissue distribution. JCI Insight. 1.

Mirzaa, G.M., et al., 2012. Megalencephaly-capillary malformation (MCAP) and megalencephaly-polydactyly-polymicrogyria-hydrocephalus (MPPH) syndromes: two closely related disorders of brain overgrowth and abnormal brain and body morphogenesis. Am J Med Genet A. 158a**,** 269-91.

Mirzaa, G.M., Riviere, J.B., Dobyns, W.B., 2013. Megalencephaly syndromes and activating mutations in the PI3K-AKT pathway: MPPH and MCAP. Am J Med Genet C Semin Med Genet. 163c**,** 122-30.

Mirzaa, G.M., Poduri, A., 2014. Megalencephaly and hemimegalencephaly: breakthroughs in molecular etiology. Am J Med Genet C Semin Med Genet. 166c**,** 156-72.
Mirzaa, G.M., et al., 2016b. Association of MTOR Mutations With Developmental Brain Disorders, Including Megalencephaly, Focal Cortical Dysplasia, and Pigmentary Mosaicism. JAMA Neurol. 73**,** 836-45.
Nakamura, K., et al., 2014. AKT3 and PIK3R2 mutations in two patients with megalencephaly-related syndromes: MCAP and MPPH. Clin Genet. 85**,** 396-8.
Negishi, Y., et al., 2017. A combination of genetic and biochemical analyses for the diagnosis of PI3K-AKT-mTOR pathway-associated megalencephaly. BMC Med Genet. 18(1):4.
Nellist, M., et al., 2015. Germline activating AKT3 mutation associated with megalencephaly, polymicrogyria, epilepsy and hypoglycemia. Mol Genet Metab. 114**,** 467-73.
Parikh, C., et al., 2012. Disruption of PH–kinase domain interactions leads to oncogenic activation of AKT in human cancers. Proceedings of the National Academy of Sciences. 109**,** 19368-19373.
Park, W.S., et al., 2008. Comprehensive Identification of PIP3-Regulated PH Domains from C. elegans to H. sapiens by Model Prediction and Live Imaging. Molecular Cell. 30**,** 381-392.
Poduri, A., et al., 2012. Somatic activation of AKT3 causes hemispheric developmental brain malformations. Neuron. 74**,** 41-8.
Riviere, J.B., et al., 2012. De novo germline and postzygotic mutations in AKT3, PIK3R2 and PIK3CA cause a spectrum of related megalencephaly syndromes. Nat Genet. 44**,** 934-40.
Slavotinek, A.M., et al., 2000. Sudden death caused by pulmonary thromboembolism in Proteus syndrome. Clin Genet. 58**,** 386-9.
Takagi, M., et al., 2017. A novel de novo germline mutation Glu40Lys in AKT3 causes megalencephaly with growth hormone deficiency. Am J Med Genet A. 173**,** 1071-1076.
Tokuda, S., et al., 2011. A novel Akt3 mutation associated with enhanced kinase activity and seizure susceptibility in mice. Human Molecular Genetics. 20**,** 988-999.
Wang, D., et al., 2013. Duplication of AKT3 as a cause of macrocephaly in duplication 1q43q44. Am J Med Genet A. 161a**,** 2016-9.
Wieck, G., et al., 2005. Periventricular nodular heterotopia with overlying polymicrogyria. Brain. 128**,** 2811-21.
Wilson, S.A., 1934. Megalencephaly. J Neurol Psychopathol. 14**,** 193-216.
Yang, Z.Z., et al., 2004. Physiological functions of protein kinase B/Akt. Biochem Soc Trans. 32**,** 350-4.

Supplementary Material

Appendix

Supplementary Table 1. Primer pairs used for site-directed mutagenesis

***AKT3* mutation**	**Forward Primer**	**Reverse Primer**
E17K	5' GGTTGGGTTCAGAAGAGGGGAAAATATATAAAAAACTGGAGG 3'	5' CCTCCAGTTTTTTATATATTTTCCCCTCTTCTGAACCCAACC 3'
N53K	5' CTTATCCCCTCAACAAGTTTTCAGTGGCAAAATG 3'	5' CATTTTGCCACTGAAAACTTGTTGAGGGGATAAG 3'
F54Y	5' CTTATCCCCTCAACAACTATTCAGTGGCAAAATGCC 3'	5' GGCATTTTGCCACTGAATAGTTGTTGAGGGGATAAG 3'
V183D	5' GAAGAAAGAAGACATTATTGCAAAGG 3'	3' CCTTTGCAATAATGTCTCTTCTTTCTTC5'
N229S	5' GATGGAATATGTTA**G**TGGGGGCGAGCTG 3'	5' CAGCTCGCCCCCA**C**TAACATATTCCATC 3'
V268A	5' CATTCCGGAAAGATTG**C**GTACCGTGATCTCAAG 3'	5' CTTGAGATCACGGTAC**G**CAATCTTTCCGGAATG 3'
D322N	5' GGTGTTAGAAGATAATAACTATGGCCGAGCAG 3'	Rev: 5' CTGCTCGGCCATAGTTATTATCTTCTAACACC 3'
R465W	5' GACAATGAGAGGTGGCCGCATTTCCC 3'	5' GGGAAATGCGGCCACCTCTCATTGTC 3'
K177M (kinase dead)	5' GAAAATACTATGCTATGATGATTCTGAAGAAAGAAG 3'	5' CTTCTTTCTTCAGAATCATCATAGCATAGTATTTTC 3'

Supplementary Table 2. Clinical and neuroimaging data of *AKT3* mutation-positive patients (N=14; this series)

DB#	LR15-262	LR16-251	LR16-372	LR16-301	LR17-100	LP96-103	LR13-041	LR14-271	LR14-254	LR12-412	LR14-025	LR12-470	LR13-008	LR14-112
Gender	M	M	F	F	M	F	F	F	F	M	M	F	M	M
Ethnicity	Caucasian	Caucasian	Hispanic	Caucasian	Caucasian	Caucasian	Caucasian	Hispanic	Caucasian	Middle Eastern	Caucasian	Hispanic	Caucasian	Caucasian
Age last assessed	2.5m	10m	8y	21m	3y	Neonatal period	3y	9m	8y10m	6y	26m	6y	6y10m	8y8m
Diagnosis	DMEG/ HMEG	DMEG/ Multifocal	MEG	MEG-PMG-PNH	MEG	MEG-PMG-PNH	MEG-PMG	MEG-PMG	MEG-PMG	MEG-PMG	MEG-PMG	MEG	MEG-autism	MEG-PMG-PNH
Birth OFC – SD	+2 SD	MEG	ND	+2.5	PENDING	ND	MEG, ND	+4	+2.5	ND	+2	ND	+2.7	Congenital MEG
Last OFC – SD (age)	–2 SD	MEG	+5 SD (8y)	+6 SD (21m)	PENDING	Postnatal MEG, ND	+4 (3y)	+ 5.5 (9m)	+6.2	+1-2 (6y)	+5 (7m)	+7-8 (6y)	+6	+2.5 (8y8m)
Digital anomalies	–	–	–	–	–	–	Mild 2-3 toe SYN	–	–	–	Partial SYN toes 3-4 (R, L)	Prominent fingertip pads	–	–
Vascular anomalies	+	+	–	–	–	–	+	–	+	–	–	–	+	+
Connective tissue anomalies	–	+	–	–	–	+	+	–	–	–	–	–	+	–
Epilepsy	+	+	–	+	–	ND	+	–	–*	+	+	–	+	+
Epilepsy onset	1h	Neonatal	–	4w	–	ND	14m	–	–	1y2m	ND	–	10h	13m

Epilepsy severity	Intractable	Intractable	–	Responsive to AED	–	ND	Multi drug resistant epilepsy	–	–	ND	ND	–	–	–
Ketogenic diet	–	+	–	–	–	ND	–	–	–	ND	ND	–	–	–
Hypoglycemia	–	+	–	–	–	ND	+	–	–	ND	ND	–	+	–
Temperature issues	–	++	–	Episodes of hyperthermia	–	ND	–	–	–	ND	–	–	Excessive sweating	–
DD/ID	NA	NA	Moderate-severe, non-verbal	Severe	–	ND	Mild	Severe early delays, poor head control	Mild-moderate	Motor delays	Mild-moderate	Mild motor delays, mild ID/LD	Mild DD	Severe GDD, no speech, wheelchair bound
Autistic features	NA	NA	+	NA	–	ND	+	NA	–	ND	–	–	ASD noted at 24-39m, – occasional self-harming behavior	–
Tone	Normal	Severe hypotonia	Infantile hypotonia	Severe hypotonia	Normal	Severe hypotonia, poor	L hemidystonia	Severe hypotonia	Mild hypotonia	Hypotonia,	Generalized	Normal	Generalized	Generalized

			(improved), hypotonic facies			head control				floppy as an infant	hypotonia		hypotonia	hypotonia
Feeding issues	NG-tube fed for 50% of feeds	Breast fed initially, then NG tube fed	+	–	–	+	Initial difficulties with dystonia	++	–	ND	Chewing difficulties	–	+, Related to hypo-/hyper-glycaemia, controlled diet	G-tube
Course	Intractable epilepsy, s/p hemispherectomy at 2w of age	Deceased at 10m 4d	Alive	Alive	Alive	Deceased, early childhood, due to pneumonia	Alive	Alive	Alive	Alive	Alive	Alive	Alive	Alive

Abbreviations: ASD, autism spectrum disorder; DD, developmental delay; DMEG, dysplastic megalencephaly; F, female; h, hour; ID, intellectual disability; LD, learning disability; M, male; m, month; MEG, megalencephaly; NA, not applicable; ND, no data; NG, nasogastric; PMG, polymicrogyria; PNH, periventricular nodular heterotopia; SYN, syndactyly; TC, tonic-clonic seizures; y, year.

Supplementary Table 3. Summary of the neuroimaging features of *AKT3* mutation positive patients identified to date (N=25)

Subject ID	Amino acid change	Domain	Type	MEG	MCD	Symmetry	VMEG HYD	CC	CBL/PF	Other MRI findings	Diagnosis
Mosaic *AKT3* mutations (N=5)											
LR15-262	p.E17K	PH	Mosaic	+	FCD2	L>>R	–	Thin, dysplastic	–	–	DMEG/HMEG
HME-1565 (Lee et al., 2012)	p.E17K	PH	Mosaic	+	FCD2	L>>R	VMEG, dysplastic ventricles	ND	ND	–	DMEG/HMEG
Patient 3(Poduri et al., 2012)	p.E17K	PH	Mosaic	+	FCD2	R>>L	–	ND	–	–	DMEG/HMEG
LR11-443(Jansen et al., 2015)	p.E17K	PH	Mosaic	+	FCD2	L>>R	VMEG	Thin, short	CBLH (mild)	Mild CBLH, increased XAX	DMEG/HMEG
LR16-251	p.E17K	PH	Mosaic	+	FCD (multifocal)	R=L	–	Thick	–	–	DMEG/multifocal
Constitutional *AKT3* mutations (by functional domain; N=20)											
Patient(Takagi et al., 2017)	p.E40L	PH	Constitutional	+	–	R=L	VMEG (mild)	–	–	–	MEG
LR16-372	p.N53L	PH	Constitutional	+	–	R=L	–	Mildly thick	–	–	MEG
LR16-301	p.F54Y	PH	Constitutional	+	Diffuse PMG-PNH	R=L	+++	Thick, stretched	–	CSPV	MEG-PMG-PNH
LR17-XXX	p.W79C	PH	Constitutional	+	–	R=L	–	–	–	–	MEG
LP96-103	p.V183D	Kinase	Constitutional	+	PMG (BPP)-PNH	R=L	VMEG (mod)	ND	–	CSPV, thin WM	MEG-PMG-PNH

LR12-314(Nellist et al., 2015)	p.V183D	Kinase	Constitutional	+	PMG (BPP)-PNH	R=L	VMEG (mild)	–	Mild CBTE	–	MEG-PMG-PNH
LR11-354(Riviere et al., 2012)	p.N229S	Kinase	Constitutional	+	PMG (BPP)	R=L	VMEG	Thick	Mild CBTE	–	MEG-PMG
Patient(Harada et al., 2015)	p.N229S	Kinase	Presumed constitutional	+	PMG (BPP)	R=L	VMEG	ND	–	CSPV	MEG-PMG
Patient 2(Nakamura et al., 2014)	p.N229S	Kinase	Constitutional	+	Diffuse PMG	L>>R	–	–	–	ND	MEG-PMG
Patient 1 (Negishi et al., 2014)	p.N229S	Kinase	Constitutional	+	PMG (BPP)	R=L	VMEG	ND	ND	–	MEG-PMG
LR13-041	p.V268A	Kinase	Presumed constitutional	+	Focal PMG (R PS)	L>R	VMEG (mod)	Mildly thick	Large CBL with mild CBTE	CSPV	MEG-PMG
LR14-271	p.D322N	Kinase	Constitutional	+	Focal PMG (L PS)	R=L	–	Mildly thick, dysplastic		–	MEG-PMG
LR14-254	p.D322N	Kinase	Constitutional	+	Focal PMG (R PS)	R=L	HYD (s/p shunt)	Thick	CBTE s/p PF decompression		MEG-PMG
LR12-412	p.R465W	C-ter	Constitutional	+	PMG (BPP)	R=L	–	Thick		Mild lumbar dural ectasia	MEG-PMG

LR14-025	p.R465W	C-ter	Constitutional	+	Diffuse PMG	R=L	VMEG (mod)	Thick	Large CBL	CSPV, increased XAX	MEG-PMG
LR12-470	p.R465W	C-ter	Presumed constitutional	+	Subtle dysgyria R PS	R=L	–	Mildly thick	–	–	MEG-autism
LR13-008	p.R465W	C-ter	Presumed constitutional	+	–	R=L	VMEG (mild)	Dysplastic, thin splenium	–	Encephalomalacia and gliosis R insular gyrus	MEG-autism
LR14-112	p.R465W	C-ter	Constitutional	+	BPP-PVNH	R=L	VMEG (mod-severe)	Mildly thick	–	–	MEG-PMG-PNH
LR08-018(Riviere et al., 2012)	p.R465W	C-ter	Constitutional	+	PMG (BPP)	R=L	VMEG (mild)	–	–	CSPV	MEG-PMG
PMG-3801(Jamuar et al., 2014)	p.R465W	C-ter	Constitutional	+	PMG	ND	ND	ND	–	ND	MEG-PMG

Abbreviations: BPP, bilateral perisylvian polymicrogyria; CC, callosal abnormalities; CSPV, cavum septum pellucidum et vergae; FCD, focal cortical dysplasia; HYD, hydrocephalus; MEG, megalencephaly; MPPH, megalencephaly-polymicrogyria-polydactyly-hydrocephalus syndrome; ND, no data; PMG, polymicrogyria; PNH, periventricular nodular heterotopia; PS, perisylvian region; VMEG, ventriculomegaly; XAX, extra-axial space.

Supplementary Table 4. Additional pertinent medical issues in patients with *AKT3* mutations

System	Patient ID	Summary
Endocrine problems		
Hypoglycemia	LR13-041	Recurrent hypoglycemia
	LR13-008	Unexplained episodes of hyper- and hypo-glycaemia. Episodes occurred particularly in the morning or if diet was not monitored. The cause of these episodes remains undetermined
		Patient LR14-254 underwent a baseline endocrine evaluation which was negative
Hypothyroidism	LR14-112	Hypothyroidism, treated with L-thyroxine
Vascular anomalies	LR15-262	Capillary malformations
	LR16-251	Patches of capillary-lymphatic malformations (~3 in number)
	LR13-041	Facial nevus flammeus and prominent veins over the abdomen
	LR14-254	Capillary malformations over the back, abdomen and thigh
	LR13-008	Prenatal stroke due to occlusion of the right anterior coronary artery, as well as capillary malformation over a patch of aplasia cutis of the cranium
	LR14-112	Patchy capillary malformations over the palms and soles bilaterally
Connective tissue abnormalities	LP96-103	Aplasia cutis congenita of the scalp
	LR13-008	Aplasia cutis congenita of the scalp
	LR13-041	Doughy skin, hypermobility
Seizures	LR15-262	Child born in status epilepticus requiring early surgery. EEG at age two days showed burst suppression activity, characterized by high amplitude bursts of spike and spike/slow wave discharges, primarily from the left hemisphere, with periods of suppressed activity. Runs of periodic rhythmic spike and spike /slow wave discharges, occurring out of primarily left hemispheres independently, during periods of amplitude suppression and sometimes representing electrographic seizures, suggestive of a severe diffuse state of cerebral dysfunction and significant cerebral hyperexcitability
	LR13-041	Focal symptomatic and tonic clonic seizures during sleep, plus astatic seizures, well-controlled on levetiracetam
	LR14-025	A few febrile convulsions with a normal EEG
	LR13-008	Focal, tonic clonic epilepsy presumed to be secondary to cerebrovascular accident, poorly controlled on trileptal
	LR14-112	Complex febrile seizures with partial secondary generalization, treated with levetiracetam, valproic acid, and phenobarbital

	LR16-251	Treated with several AEDs
	LR16-301	General and focal, generalized tonic-clonic seizures, controlled on several AEDs. Seizure activity on EEG. Spasm controlled on vigabatrin and corticosteroids.
	*LR14-254	EEG epileptic abnormalities including centro-temporal bilateral asynchronous slow waves, with activation during slow sleep during the last two years of age
Other medical issues	LR14-271	Failure to thrive
	LR12-412	Short stature
	LR14-025	Excessive oral secretions, signs of supra-bulbar palsy
	LR13-008	Severe vitamin A malabsorption
	LR14-112	IgA and IgE deficiency with susceptibility to severe infections
	LR13-041	Recurrent infections

Supplementary Table 5. Molecular finding, levels of mosaicism and detection method of *AKT3* mutation positive patients identified to date (N=25).

Subject ID	cDNA change	Amino acid change	Type	Alternative allele fraction (AAF)	Inheritance	Method of detection
Mosaic *AKT3* mutations						
LR15-262	c.49G>A	p.Glu17Lys	Mosaic	0%^{blood}, 12.6-13.9%^{brain}, 8.6-9.5%^{FB}	NA	Multiplex PCR, NGS v.1 IonTorrent
HME-1565 (Lee et al., 2012)	c.49C>T	p.E17K	Mosaic	~16-30%	*De novo*	PCR-restriction endonuclease enzyme assay
Patient 3(Poduri et al., 2012)	c.49G>A	p.Glu17Lys	Mosaic	35%^{brain} 0%^{blood}	*De novo*	Sanger sequencing, topo-cloning
LR11-443(Jansen et al., 2015)	c.49G>A	p.Glu17Lys	Mosaic	10-18%^{brain}, 0%^{dura}, 10/779 (1.3%)^{FB}	*De novo*	MIPs, Sanger sequencing
LR16-251	c.49G>A	p.Glu17Lys	Mosaic	15/779 (1.8%)^{FB}	NA	Targeted NGS
Constitutional *AKT3* mutations						
Patient(Takagi et al., 2017)	c.118G>A	p.Glu40Lys	Constitutional	56/114 (49.1%)^{blood}	*De novo*	WES
LR16-372	c.159C>A	p.Asn53Leu	Constitutional	~50%^{blood}	*De novo*	WES (singleton, with parental Sanger confirmation)
LR16-301	c.161T>A	p.Phe54Tyr	Constitutional	~50%^{blood}	*De novo*	WES (singleton, with parental Sanger confirmation)
LR17-XXX	c.237G>T	p.Trp79Cys	Constitutional	492/1023 (48%) ^{blood}	*De novo*	Targeted NGS
LP96-103	c.548T>A	p.Val183Asp	Constitutional	291/556 (52%)^{blood}	*De novo*^{blood}	MIPs, Sanger sequencing
LR12-314(Nellist et al., 2015)	c.548T>A	p.Val183Asp	Constitutional	144/301 (48%)$^{blood/FB}$	*De novo*	MIPs, Sanger sequencing
LR11-354(Riviere et al., 2012)	c.686A>G	p.Asn229Ser	Constitutional	~50%^{blood}	*De novo*^{blood}	Sanger sequencing

Patient(Harada et al., 2015; Nakamura et al., 2014)	c.686A>G	p.Asn229Ser	Presumed constitutional	~50%^{blood}	*De novo*	Targeted NGS, Sanger sequencing
Patient 1 (Negishi et al., 2014)	p.N229S	Kinase	Constitutional	~50%^{blood}	*De novo*	WES
Patient 2(Nakamura et al., 2014)	c.686A>G	p.Asn229Ser	Constitutional	52.5%^{blood}	*De novo*	WES
LR13-041	c.803T>C	p.Val268Ala	Presumed constitutional	158/320 (49%)^{blood}, 10/29 (34%)^{saliva}	*De novo*$^{blood, saliva}$	MIPs, Sanger sequencing
LR14-271	c.964G>A	p.Asp322Asn	Constitutional	436/874 (50%)^{blood}	*De novo*^{blood}	NGS
LR14-254	c.964G>A	p.Asp322Asn	Constitutional	~50%^{saliva}	*De novo*^{saliva}	NGS (Haloplex), Sanger sequencing
LR12-412	c.1393C>T	p.Arg465Trp	Constitutional	50%^{blood}	NA	MIPs, Sanger sequencing
LR14-025	c.1393C>T	p.Arg465Trp	Constitutional	50%^{blood} 50%^{saliva}	*De novo*$^{blood, saliva}$	MIPs, Sanger sequencing
LR12-470	c.1393C>T	p.Arg465Trp	Presumed constitutional	11/34 (32%) ^{saliva}	*De novo*^{saliva}	MIPs, Sanger sequencing
LR13-008	c.1393C>T	p.Arg465Trp	Presumed constitutional	8/23 (35%)^{saliva}	*De novo*^{saliva}	MIPs, Sanger sequencing
LR14-112	c.1393C>T	p.Arg465Trp	Constitutional	50%^{blood,} 50%^{saliva}	*De novo*^{saliva}	MIPs, Sanger sequencing
LR08-018(Riviere et al., 2012)	c.1393C>T	p.Arg465Trp	Constitutional	43%^{blood}	*De novo*	WES, Sanger sequencing
PMG-3801(Jamuar et al., 2014)	c.1393C>T	p.Arg465Trp	Constitutional	22/50 (44%)^{blood1}	*De novo*	MIPs, Sanger sequencing

Abbreviations: FB, skin fibroblasts; NGS, next generation sequencing; MIPs, molecular inversion probes; WES, whole exome sequencing.

AKT3: **NM_005465.4**

Supplementary Table 6. Fisher's exact test comparing the association between segmental cortical malformations and the type of *AKT3* mutation (mosaic vs. constitutional).

Cohort	Segmental cortical malformations (FCD/HMEG)	No segmental cortical malformations	Total
Mosaic *AKT3* mutations (E17K)	**5**	**0**	**5**
Constitutional *AKT3* mutations (all others)	**0**	**20**	**20**
Total	**5**	**20**	**25**
The two-tailed P value <0.0001 (extremely statistically significant)			

Figure

Supplementary Figure. Proposed diagnostic workflow for individuals with megalencephaly (MEG). Individuals with megalencephaly can be clinically stratified based on several features, including brain imaging abnormalities, into several groups including individuals with highly focal malformations of cortical development (such as focal cortical dysplasia, FCD, hemimegalencephaly, HMEG) caused by mosaic mutations of the PI3K-AKT-MTOR pathway (group 1); individuals with polymicrogyria (with or without heterotopia; group 2); and individuals with diffuse megalencephaly but without the consistent cortical dysplasia (seen more commonly in groups 1 and 2).

Notes: *Other PI3K-AKT-MTOR pathway genes (such as *PTEN*) may be associated with these disorders as well.
**Polymicrogyria in this group is typically bilateral perisylvian in distribution.
***This is a highly heterogeneous group of disorders that can also be associated with characteristic brain malformations in some individuals. Several of these syndromes are also associated with somatic overgrowth (gene in **bold text**).

Supplementary Text

Additional pertinent medical information:

Patient LR16-301: This child had severe hypotonia at birth. Seizures first occurred at 4 weeks of age. Infantile spasms (ISS) occurred at 3 months of age. During the first year of life, this child was noted to have many episodes of discomfort with crying and arching of the back. She also had episodes of suspected high intracranial pressure (ICP). Furthermore, this child had episodes of hyperthermia of unexplained etiology. The first episode lasted 4 weeks and was partially responsive to Propranolol. This child has global developmental delays. She is non-verbal. She recognizes family members and is fond of patterns and music. She eats a general diet by mouth and has been growing well. The episodes of discomfort have decreased dramatically during the second year of life.

Patient LR14-025: This child walked at 20 months of life. He has delayed speech and is non-verbal at 20 months of age.

Patient LR12-470: This girl has mild/borderline intellectual disability with communicative disability that did not meet classic criteria for Autism Spectrum Disorder (ASD). She also has significant behavioral issues with temper tantrums and sleep difficulties as well.

Patient LR13-008: This child walked at approximately 18 months of age. He had no speech development. Cognitive assessments around 5 years of age identified his cognitive level to be 18 months of age. His eye contact deteriorated around 2.5 years of age and he was formally diagnosed with Autism Spectrum Disorder (ASD).

Patient LR16-251: This child passed away due to complications from chronic intractable epilepsy. At 10 months of age, he had progressive feeding intolerance requiring a reduction in his feeding volumes.

Patient LR14-254: Psychomotor delays. At 24 months, His Griffiths Mental Development scale (GQ) was 62. At 6 years of age, his WPPSI-III scores were as follows: QIT= 92, QIV=94, QIP=100.

Patient LR08-018: This boy was born at 38 weeks of gestation because of maternal hypertension. Delivery was by Cesarean section because of failure-to-progress. His birth weight was 8 pounds, 3 ounces, and his OFC was 38.5 cm (+2.5 standard deviations, SD). His Apgar scores were 9 and 9. He was followed closely after discharge because of his large head size and found to have a mildly weak suck, hypotonia, and subtle right-sided tremors that were not associated with epileptic discharges on EEG. Brain imaging studies - serial ultrasound, head CT and brain MRI - showed large brain, enlarged but asymmetric ventricles and a cortical malformation that appeared more extensive on the left side. A small vascular malformation was seen beneath his umbilicus.

By age 3 months, he had intermittent stridor, gastroesophageal reflux, constipation, and rapidly enlarging head size. Throughout his first years of life, his head grew rapidly with his OFC measured at +4 SD by 3 months, +5 SD by 5 months, and +6 SD by 11 months of age. Serial brain imaging studies revealed hydrocephalus and mild cerebellar tonsils herniation (not quite Chiari malformation) and a shunt was placed at 11 months of age. His parents thought that his development improved after the shunt.

Examination showed a markedly enlarged head with prominent forehead and prominent small veins over his forehead, mildly deep-set eyes, wide and prominent forehead, prominent fleshy soft tissues of his face, high-arched palate, everted lower lip and prominent

dimple. His skin felt soft and doughy suggesting a subtle connective tissue dysplasia. He had mildly diminished movements and increased tone on his right side.

By age 3 years, he had made some developmental progress. He had had two short seizures. He was non-verbal but could use communicate by touching pictures on a computer screen. By 4 years, he could walk, use about 20 single words, and follow simple commands. He also had onset of seizures that became progressively more frequent and severe. These included series of myoclonic jerks lasting up to 30 minutes, asymmetric generalized tonic-clonic seizures that were more severe on his right side and lasted 1-5 minutes, and a few episodes of unresponsiveness lasting 5-8 minutes. Most occurred in the morning soon after waking, often with an aura as he would walk toward his parents just before they began. Trials of multiple seizure medications had little effect, but the ketogenic diet reduced seizure frequency to 1-2 per week.

In the weeks before his death, his seizure frequency had increased but he was otherwise healthy. On the day before his death he went to sleep at his usual time and was seen breathing normally in the late evening. His parents found him unresponsive and not breathing but still warm early the following morning, and he could not be resuscitated. While the terminal event was not witnessed, his history of intractable epilepsy and recent increase in seizures suggest sudden unexpected death in epilepsy (SUDEP).

His growth measurements throughout life were the following:

Age	**Size (cm)**	**Size (SD)**
Birth	38.5 cm	+1.63
2.5 months	46 cm	+4.2
4 months	47.5	+4.5
5 months	49.5	+5.25
11 months	54	+6

References

Harada, A., et al., 2015. Sudden death in a case of megalencephaly capillary malformation associated with a de novo mutation in AKT3. Childs Nerv Syst. 31**,** 465-71.

Jamuar, S.S., et al., 2014. Somatic mutations in cerebral cortical malformations. N Engl J Med. 371**,** 733-43.

Jansen, L.A., et al., 2015. PI3K/AKT pathway mutations cause a spectrum of brain malformations from megalencephaly to focal cortical dysplasia. Brain. 138**,** 1613-28.

Nakamura, K., et al., 2014. AKT3 and PIK3R2 mutations in two patients with megalencephaly-related syndromes: MCAP and MPPH. Clin Genet. 85**,** 396-8.

Nellist, M., et al., 2015. Germline activating AKT3 mutation associated with megalencephaly, polymicrogyria, epilepsy and hypoglycemia. Mol Genet Metab. 114**,** 467-73.

Poduri, A., et al., 2012. Somatic activation of AKT3 causes hemispheric developmental brain malformations. Neuron. 74**,** 41-8.

Riviere, J.B., et al., 2012. De novo germline and postzygotic mutations in AKT3, PIK3R2 and PIK3CA cause a spectrum of related megalencephaly syndromes. Nat Genet. 44**,** 934-40.

Takagi, M., et al., 2017. A novel de novo germline mutation Glu40Lys in AKT3 causes megalencephaly with growth hormone deficiency. Am J Med Genet A.